Investigation on Co–Modified Ni_xMg_yO Solid Solutions for Hydrogen Production from Steam Reforming of Acetic Acid and a Model Blend

Xiang Luo, Yu Hong, Kaiqi Shi, Gang Yang, Chengheng Pang, Edward Lester, Lei Jiang, Tao Wu

University of Nottingham Ningbo China, 199 Taikang East Road, Ningbo, 315100, Zhejiang, China.

First published 2019

University of Nottingham
UK | CHINA | MALAYSIA

Investigation on Co-Modified Ni_xMg_yO Solid Solutions for Hydrogen Production from Steam Reforming of Acetic Acid and a Model Blend

Dr. Xiang Luo,[a], [b] Dr. Yu Hong,[a], [c] Dr. Kaiqi Shi,[a] Mr. Gang Yang,[a] Dr. Chengheng Pang,[a], [c] Prof. Edward Lester,[d] Ms. Lei Jiang,[d] Prof. Tao Wu*[a],[b]

[a] New Materials Institute, The University of Nottingham Ningbo China, Ningbo 315100, PR China

[b] Municipal Key Laboratory of Clean Energy Conversion Technologies, The University of Nottingham Ningbo China, Ningbo 315100, PR China

[c] Department of Chemical and Environmental Engineering, The University of Nottingham Ningbo China, Ningbo 315100, PR China

[d] Department of Chemical and Environmental Engineering, The University of Nottingham, University Park, Nottingham NG7 2RD, UK

Corresponding author: tao.wu@nottingham.edu.cn

Abstract

This paper is focused on the Co-modified Ni_xMg_yO solid solutions (10wt% Ni, 2-6wt% Co) for the steam reforming of acetic acid and a model blend. The pristine rocksalt structured Ni_xMg_yO solid solution and the modified Ni_xMg_yO-Co catalysts were synthesized via hydrothermal method and co-impregnation. The activity of the catalysts was evaluated in the temperature range of 500-800 °C with a steam/carbon molar ratio of 3 and a gas hourly space velocity (*GHSV*) of 57,000 h^{-1}. Low cobalt content (Co loading = 2wt%) catalysts exhibited significant promotion of H_2 yield via enhancement of both water-gas shift (WGS) reaction and methane decomposition. A 30-hour test at 700 °C achieved excellent acetic acid conversion rate and H_2 yield of 99.1% and 86.9%, respectively. However, the catalysts with higher cobalt loading (Co loading ≥ 4wt%) suffered a much quicker deactivation mainly due to carbon deposition. In addition, the catalysts were also tested on a model blend combined acids, alcohols and aromatic species and exhibited

outstanding performance with carbon conversion above 90% and H_2 yield above 70% for 100 h.

Introduction

Biomass gasification followed by water-gas shift (WGS) reaction is a natural option for the production of hydrogen from biomass.[1] However, this approach is not economically feasible since biomass has a very low volumetric energy density, which makes it impractical for long distance transportation and hinders its large-scale and highly-efficient utilization. Bio-oil is obtained from the fast pyrolysis of biomass, the energy density of which is approximately 10 times of that of biomass.[2] The pyrolysis unit could also be deployed at the place where feedstock is readily available to produce bio-oil that is more practical for long distance transportation and therefore to make large-scale utilization of biomass possible. Hence, numerous researches have been conducted on hydrogen production from bio-oil catalytic steam reforming.

Normally, steam reforming of bio-oil involves the reforming of a series of oxygenated hydrocarbons. The complete chemical reaction can be expressed as following:[3]

$$C_nH_mO_k + (n-k)\ H_2O \rightarrow n\ CO + (n + m/2 - k)\ H_2 \qquad (R1)$$

$$CO + H_2O \rightarrow CO_2 + H_2 \qquad (R2)$$

In the 1990s, catalyst development attracted considerable research efforts, especially the broad application of Ni-Al_2O_3-based catalysts.[4] Active metal nickel shows a great activity towards the C-C bond cleavage. However, in actual reforming system, the direct cleavage leads to the formation of coke:

$$C_nH_mO_k \rightarrow C_xH_yO_z + \text{gas products } (H_2, CO, CO_2, CH_4\ldots) + \text{coke} \qquad (R3)$$

It is found that addition of alkali metals or alkaline earth metals could promote catalyst surface water adsorption, and therefore accelerate coke gasification.[5] In addition, researchers also investigated bimetallic system, such as Ni-Co, Ni-Mo, Ni-Fe, Ni-Sn, and Ni-Cu, in which metal additives could prevent carbon formation by blocking step sites over

nickel particles.[6, 7] It is therefore of considerable interest to employ some nature minerals and ash materials, which are rich in alkali, alkaline earth metal oxides and other transition metals, as catalyst precursors for steam reforming. Recent research on nickel-based catalysts also showed performance of catalyst is also dependent on precursors,[8] nickel loading[9] and structure of the catalyst.[10]

Normally, most of the research on hydrogen production from bio-oil is carried out by looking at the steam reforming of bio-oil model compounds including acetic acid, acetone, ethanol, phenol and glycerol. This is due to the complex distribution of components changes with the biomass precursor and pyrolysis parameters. Acetic acid (HAc) is one of the major carboxylic acid compounds in bio-oil with a concentration up to 10-12wt%.[11-14] Hydrogen production from steam reforming of HAc leads to the formation of H_2 between 70-80%.[15-17] The overall reaction is the combination of steam reforming of HAc and WGS reaction:

$$CH_3COOH + 2\ H_2O \rightarrow 2\ CO_2 + 4\ H_2 \qquad \text{(R4)}$$

Mechanism of the steam reforming of HAc is shown below:[18]

$$CH_3COOH + 2* \rightarrow CH_3COO* + H* \qquad \text{(R5)}$$

$$CH_3COOH + 2* \rightarrow CH_3CO* + OH* \qquad \text{(R6)}$$

The adsorption of HAc over catalyst surface was identified as the first step, which involves the decomposition of HAc into acetate or acyl species.[19] The acetate and acyl would further decompose into CO_2, CO and CH_x-species ($X \leq 4$). Thermodynamic studies indicated that both the ratio of steam to HAc and the operating temperature are two primary factors that could significantly affect hydrogen production and coke formation.[12] However, more steam input lowers the overall efficiency of the reforming process. For the effect of temperature, the rate of hydrogen production increases gradually with temperature in the region of 127-627 ℃ before dropping slightly with further climbing to 1027 ℃.[12] This adverse effect at high temperature region is attributed to moderate exothermic property of WGS reaction.[20] Thus, proper design of catalyst capable for WGS

reaction promotion, above 400 ℃, will be a major target for future research.[21, 22] For high temperature shift, Co-based catalysts has been widely studied due to its high activity and sulfur tolerance.[23] Thus, a series of Co-modified nickel catalysts were tested at 500-800 °C, which demonstrated that optimal catalytic performance could be achieved via easily control of catalysts component.[24-27] Recent research over $Ni_xCo_{1-x}MgO_6O_{7\pm\delta}$ showed that optimal ratio of Ni and Co can suppress the oxidation of Ni^0 and Co^0 and avoid quick deactivation of catalysts. However, high CO selectivity of 30% indicated that hydrogen yield of 80% could be further promoted with WGS reaction enhancement.[28]

In this paper, we employed Co-modified Ni_xMg_yO solid solution as the catalyst for steam reforming of acetic acid as well, while the preparation method of catalysts was conducted with extra hydrothermal treatment. The effect of cobalt loading over WGS reaction promotion and methane decomposition was investigated. The optimal composition of the catalyst was determined together with appropriate operating conditions and material characterization. Moreover, the test of catalysts durability was carried out in the steam reforming of a bio-oil model blend to explore its potential for commercial application. Pure acetic acid, ethanol, and phenol were used to simulate the presence of acids, alcohols, and aromatic species to prepare a water-free model bio-oil ($C_{4.74}H_{8.00}O_{2.07}$).[29]

Results and discussion

Characteristic of fresh catalysts

Table 1 shows the composition of catalysts as determined by ICP-AES. Nickel content of the four catalysts are controlled at the range between 8.2 and 8.6%. The cobalt content of three catalysts were found to be 1.7, 3.4 and 5.2%, respectively. The proportion of these measured content is also consistent with the theoretical value. The isotherm curves and the porosity feature of the catalysts is shown in Fig. 1 (a) and (b). The type of isotherm curves of four catalysts can be categorized as Pseudo-Type II, which suggests the existence of slit-shaped pores or aggregates of platy particles.[30] For all the catalysts, the pore width varies from 3 to 5 nm. In addition, the size of the hysteresis loops in Fig.1 (a)

also confirms that the addition of cobalt reduces the quantity of small pores due to the blockage of some pores.

Table 1

Elemental analysis results of the catalysts.

Catalyst	Theoretical composition			Measured composition[a]			Surface area (m^2/g)
	Ni	Co	MgO	Ni	Co	Mg	
Ni_xMg_yO	10.0%	N/A	90.0%	8.4%	N/A	51.7%	56
Ni_xMg_yO-2Co	10.0%	2.0%	88.0%	8.2%	1.7%	45.4%	46
Ni_xMg_yO-4Co	10.0%	4.0%	86.0%	8.3%	3.4%	47.3%	30
Ni_xMg_yO-6Co	10.0%	6.0%	84.0%	8.6%	5.2%	44.7%	30

[a] Measured by ICP-AES for the bulk composition, balanced by oxygen.

The XRD patterns of fresh catalysts were collected to study their crystalline structures, shown in Fig. 1 (c). For the Ni_xMg_yO catalyst, the five typical diffraction peaks without double-peak structure indicated the formation of the rocksalt structured Ni_xMg_yO solid solution.[31, 32] This is due to the same valence number and the close ionic radius of Ni^{2+} and Mg^{2+}.[33] While, the fresh Co-modified catalysts had similar patterns with the Ni_xMg_yO catalyst, which was also attributed to the close ionic radius and identical lattice type of Co^{2+} and Ni^{2+}. Thus, the excellent mutual solubility of Co, Ni and Mg led to the formation of a stable solid solution structure.

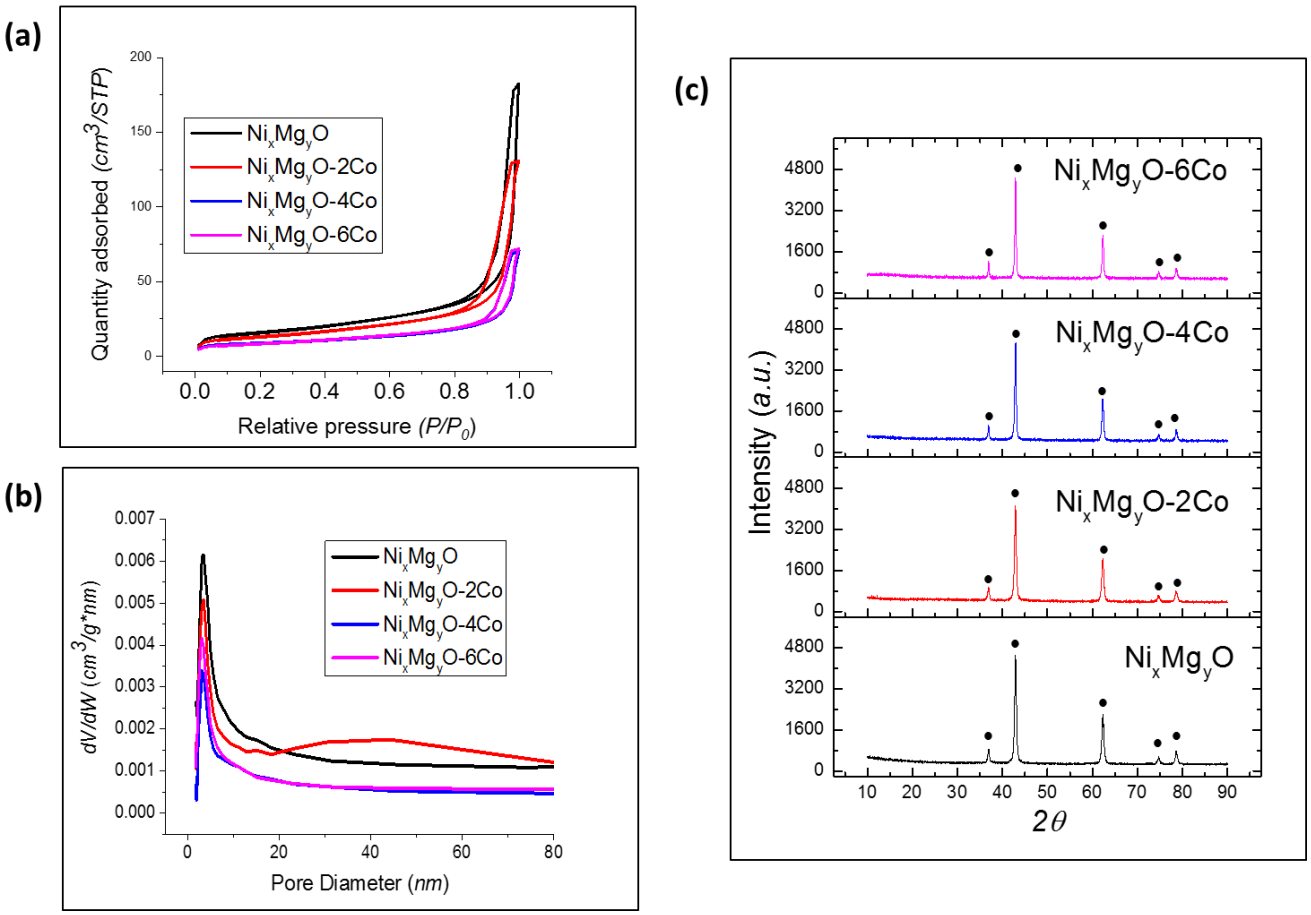

Fig. 1. (a) N_2 adsorption-desorption isotherms of the fresh catalysts; (b) the pore size distribution of the fresh catalysts; (c) X-ray diffraction patterns of fresh catalysts.

Fig. 2 (a) shows the H_2-TPR profiles of the four catalysts. The main hydrogen consumption peak of the pristine Ni_xMg_yO catalyst was at 890 °C, which was attributed to the reduction of the oxidized nickel from the MgO matrix.[34] This finding confirmed the formation of the Ni_xMg_yO solid solution, which was consistent with the results of XRD analysis. For the Co-modified catalysts, two representative peaks can be recognized at 170 and 890 °C. The small humps around 170 °C were previously identified as the consumption of free oxygen connected with the Ni_xMg_yO facets or partial reduction of Co_3O_4,[35, 36] while the hydrogen consumption peaks around 890 ℃ were related to the reduction of Ni^{2+} dissolved deep in the MgO lattice or complete reduction of $MgCo_2O_4$.[37] It is also worth noting that the reduction peak area of the Co-modified catalysts decreased with the increasing of cobalt doping. Due to the co-impregnation of nickel and cobalt in the process of catalyst preparation, the synergic effect between nickel and cobalt lowered the reducibility of the catalysts. The surface nickel states were also investigated by using XPS technique, as

shown in Fig. 2. For both reduced catalysts, no Ni^0 was observed because reducing Ni^{2+} in the Ni-O-MgO sites requires a temperature above 700 ℃. This was also confirmed by H_2-TPR results. Compared the two types of catalysts, the cobalt modified catalyst showed a substantial attenuation on the intensity of the Ni 2p without peaks shift, which is due to the shielding effect of cobalt addition.

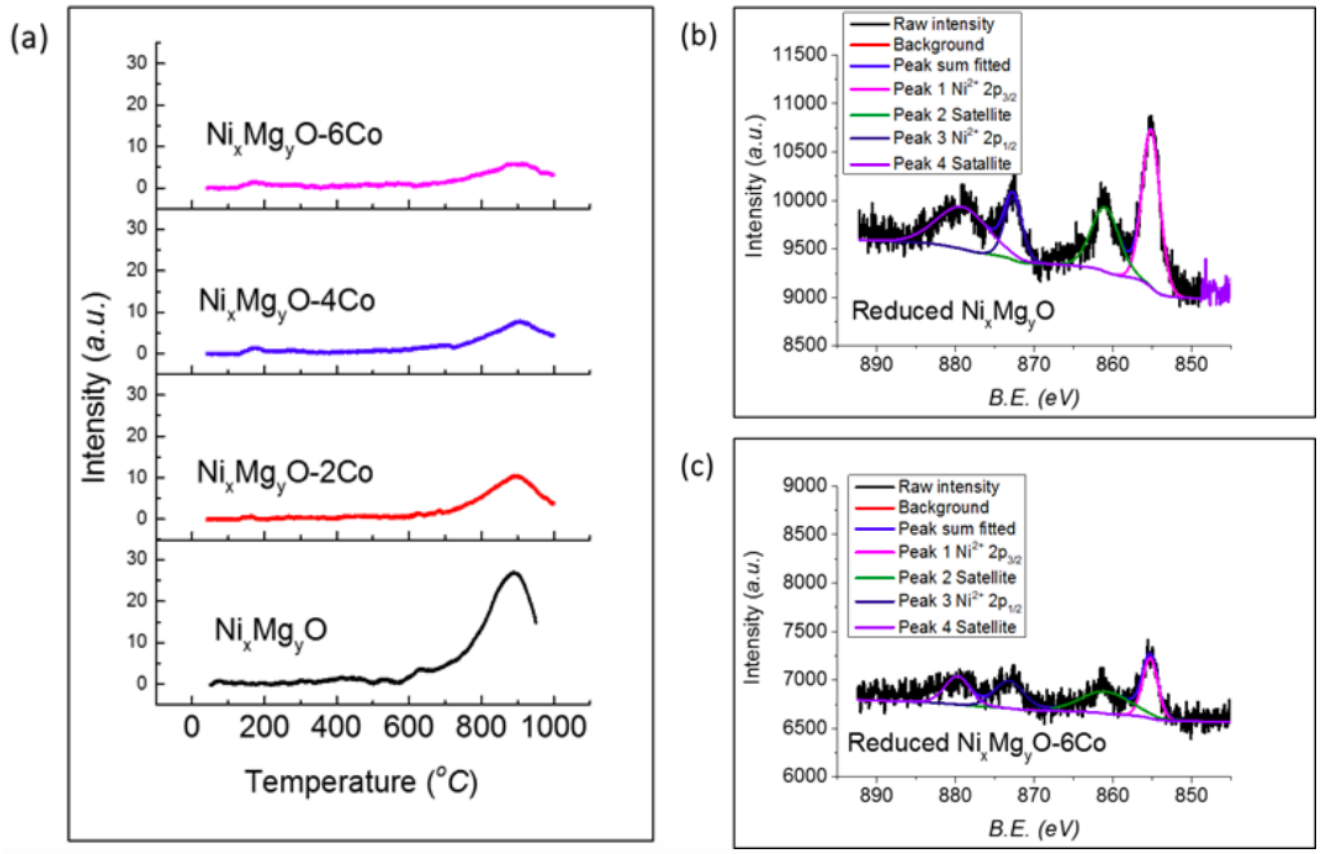

Fig. 2. (a) H_2-temperature programmed reduction profiles of fresh catalysts; (b) Ni 2p spectra of the reduced Ni_xMg_yO catalyst; (c) Ni 2p spectra of the reduced Ni_xMg_yO-6Co catalyst.

Fig. 3 shows the TEM images of all the catalysts. The Ni_xMg_yO catalyst exists as nano-particles whereas for the Co-modified catalysts, particles start to merge into each other with the increase in cobalt loading. This may help explain the affinity between Ni and Co clusters.

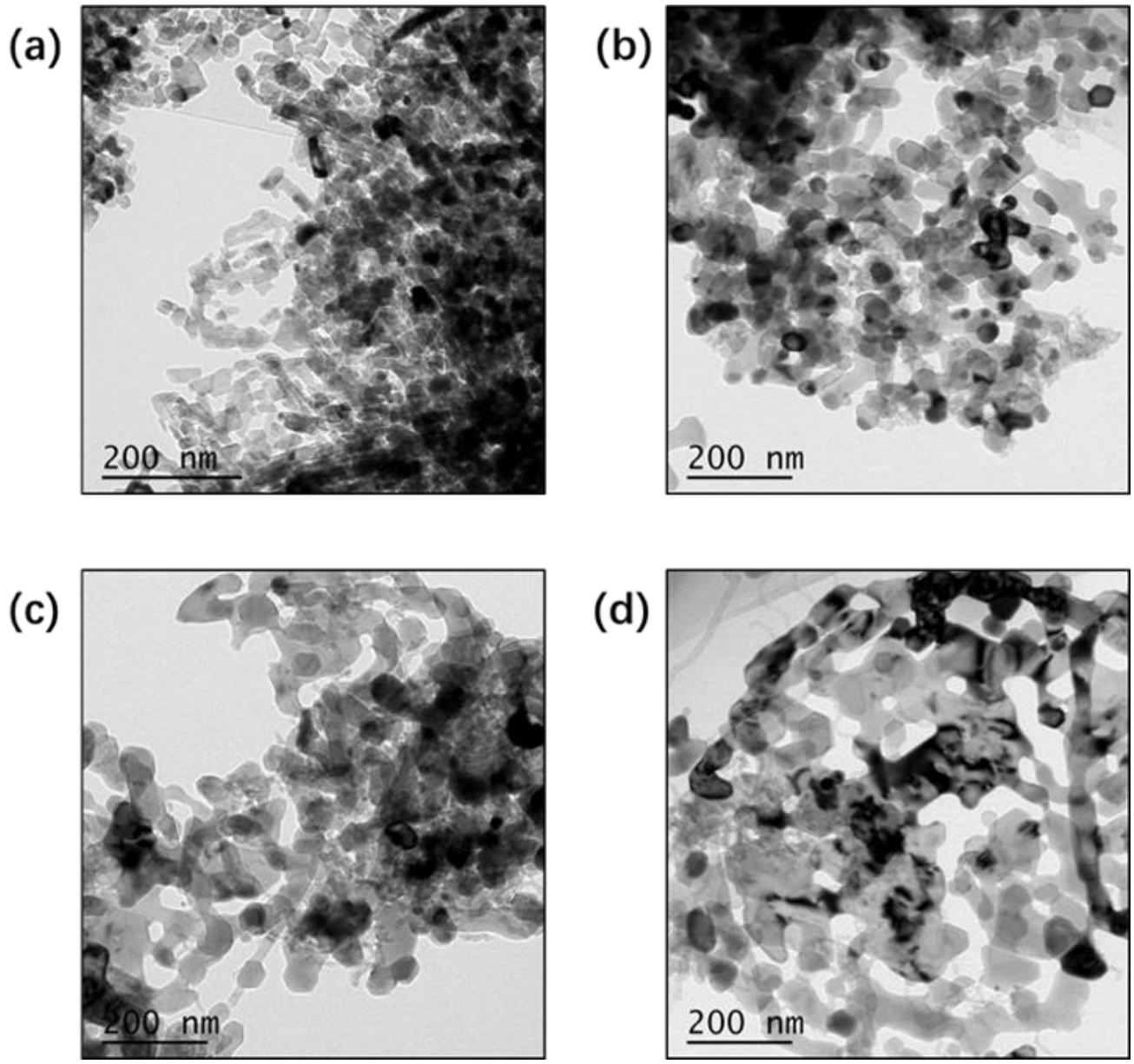

Fig. 3. TEM images for the fresh catalysts (a)Ni_xMg_yO; (b) Ni_xMg_yO-2Co; (c) Ni_xMg_yO-4Co; (d) Ni_xMg_yO-6Co.

Steam reforming of acetic acid

Effect of cobalt loading and temperature

The effect of cobalt loading (from 0.0 to 6.0 wt%) on the steam reforming of HAc was investigated over the Ni_xMg_yO solid solution. The gas yield and HAc conversion as a function of temperature (from 500 to 800 °C) are displayed in Fig. 4. It can be seen that temperature has significant influence on H_2 yield and carbon conversion, as shown in Fig. 4 (a) and (b). Taking the Ni_xMg_yO catalyst as an example, its H_2 yield increased from 13.3%

at 500 °C to 55.5% at 600 °C, and reached 80.4% as the peak value at 700 °C. This is due to the endothermic nature of HAc reforming.[3] However, the H_2 yield dropped to 60.0% when temperature was further raised to 800 ℃. The reason for this behavior is that WGS reaction was inhibited at that high temperature, as previously discussed. This performance is also similar as the results obtained by others that a similar Ni-based catalyst supported on mesoporous MgO was employed in the steam reforming of HAc.[38] The carbon conversion rate of the Ni_xMg_yO catalyst followed a similar trend as the H_2 yield and showed an initial conversion rate of 15.6% at 500 ℃ and then 99.9% when temperature was raised to 800 °C.

For the other three catalysts with different cobalt loading, the Ni_xMg_yO-2Co and the Ni_xMg_yO-4Co catalysts exhibited higher hydrogen productivities than the unmodified Ni_xMg_yO catalyst. At 600 °C, the H_2 yields of these two catalysts were 65.5% and 71.0%, respectively. When temperature increased to 700 ℃, their H_2 yields further increased by 22.3% and 16.3% correspondingly. At 800 °C, the H_2 yields of both catalysts were still above 84.0%, which was about 24.0% higher than that of the Ni_xMg_yO catalyst. It could be concluded that the Ni_xMg_yO catalyst with a small quantity of cobalt loading ($\leq$ 4wt%) could significantly promote H_2 yield in steam reforming of HAc. However, a higher cobalt loading led to a deteriorated catalytic activity. The Ni_xMg_yO-6Co catalyst showed the lowest hydrogen productivity at all the temperature levels tested.

Fig. 4 also illustrated the influence of temperature over the yield of three major gas compounds (CO_2, CO and CH_4). It is generally the case that gas yields increased with temperature. But when temperature was raised from 700 to 800 °C, the CO_2 yield of the Ni_xMg_yO decreased from 71.1% to 63.0%, while the CH_4 yield increased dramatically from 2.0% to 15.1%. In the meantime, the CO yield of the Ni_xMg_yO catalyst almost remained unchanged. When temperature increased, the decomposition of acetate or aryl species would be enhanced thermodynamically to produce more methane. However, the WGS reaction and the steam reforming of methane were both suppressed and consequently reduced H_2 yield and CO_2 yield. For the Ni_xMg_yO-2Co and the Ni_xMg_yO-4Co, it can be seen

that the both catalysts had higher CO_2 yield but lower CO yield by comparing with the yields of the pristine Ni_xMg_yO at all the investigated temperature ranges. Such higher CO_2 selectivity indicated that better H_2 yield was due to enhancement of WGS reaction. Secondly, the CH_4 yields of the both catalysts were also controlled at a lower level. It can be concluded that low cobalt doping also promoted the steam reforming of methane, which further increased hydrogen selectivity.

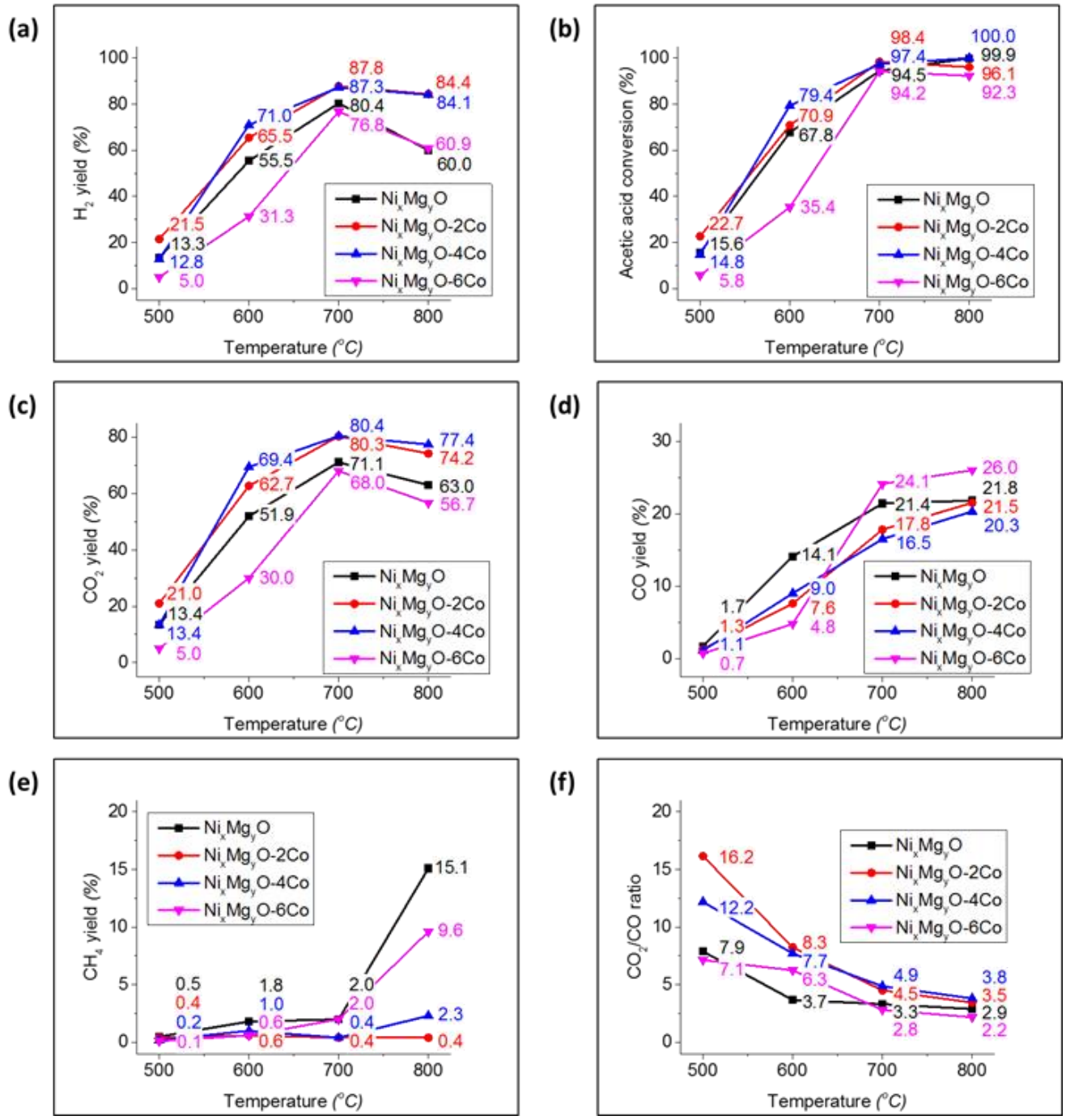

Fig. 4. Catalysts performance over steam reforming of acetic acid as a function of temperature (reaction condition: *P* = 1 atm, *GHSV* = 57,000 h^{-1}, *S/C* = 3).

Effect of time on stream

The durability of the catalysts was also investigated by carrying out long-term tests for 30 h. In Fig. 5 (a), the unmodified Ni_xMg_yO catalyst, however, showed a deactivation of HAc conversion with 12.8% decrement from 94.5 to 81.7% after 30 h. While the H_2 yield of the Ni_xMg_yO catalyst suffered a much severe attenuation, it dropped by 18.5% from 80.4 to 61.9%. The deactivation is normally attributed to the carbon deposition and the active metal sintering.[39] The deposited carbon would encapsulate the active metal sites to stop the reaction, while the growing active metal particles would lead to a decreasing of active surface. However, the decrement of H_2 yield was also contributed by attenuation of WGS reaction. This speculation is supported by the fact that CO_2 yield decreased dramatically after 10 h while the CO yield increased reversely. In Fig. 5 (c) and (d), both the Ni_xMg_yO-4Co and the Ni_xMg_yO-6Co catalysts showed even more severe deactivation, especially the Ni_xMg_yO-6Co, which only demonstrated a H_2 yield of 10.6% after 30 h.

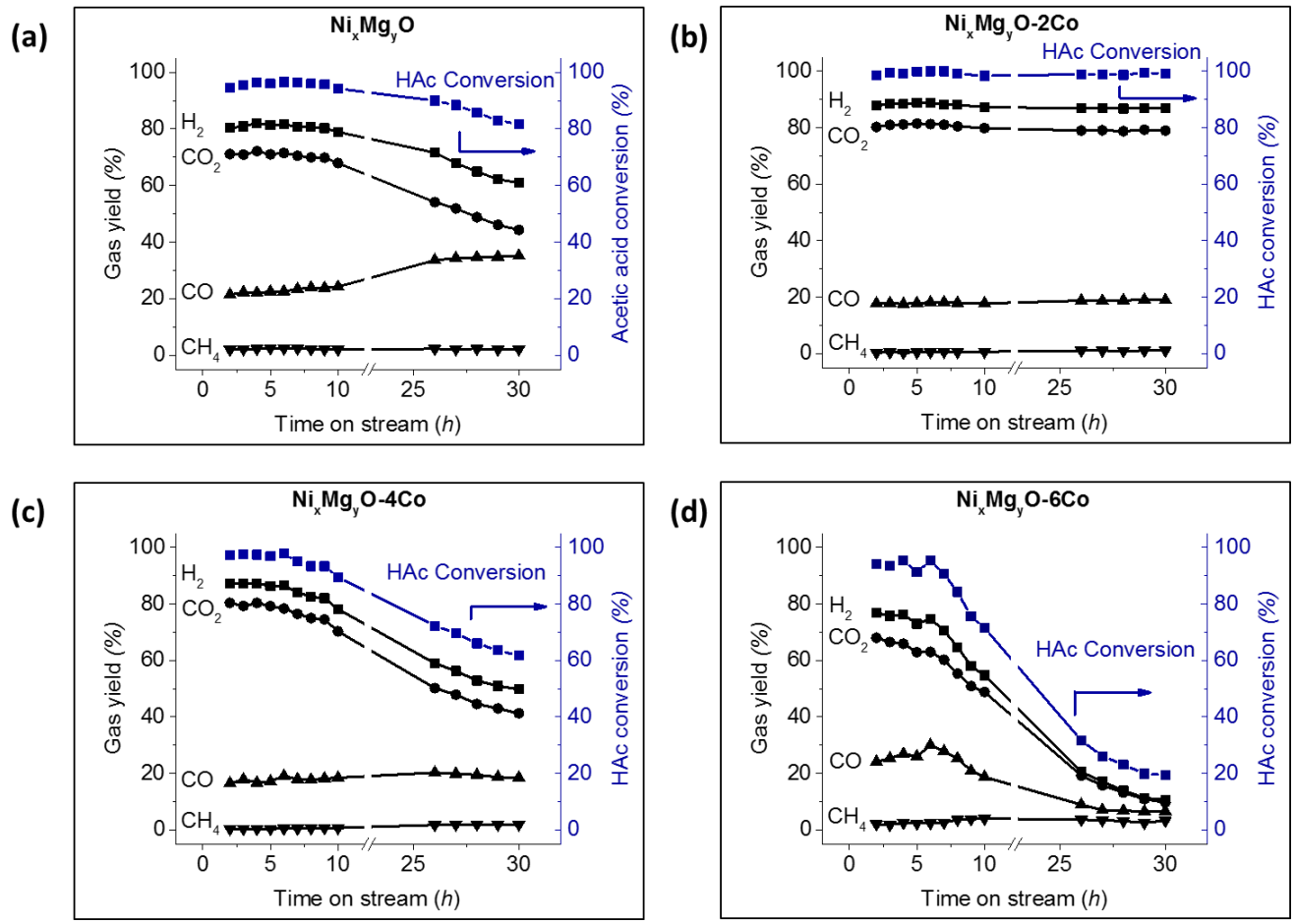

Fig. 5. Acetic acid conversion and gas yields profiles of catalysts as a function of time in the durability tests (reaction condition: P = 1 atm, $GHSV$ = 57,000 h^{-1}, S/C = 3, T = 700 ℃).

Taking into account the performance of the Ni_xMg_yO-2Co as shown in Fig. 5 (b), it showed that the yields of all the gas components were kept very stable. The catalyst illustrated an outstanding performance with a final H_2 yield of 86.9% and a HAc conversion of 99.1%. For the other gas components, the CO_2 yield was around 80% and the CO yield was controlled slightly lower than 20% during the whole test period. These results indicated that the WGS reaction was maintained to ensure a high productivity of hydrogen. On the other hand, the CH_4 yield was also limited below 1%, which can be attributed to high-efficiency steam reforming of methane. Table 2 shows the comparison between the Ni_xMg_yO-2Co catalyst and the selected catalysts.[18] It fully embodies the excellent and competitive performance of the Ni_xMg_yO-2Co catalyst. In summary, cobalt addition could promote the initial activity of the Ni_xMg_yO catalysts in steam reforming of HAc, whereas high doping level (≥ 4wt%) normally leads to a fast deactivation over time. The most

valuable finding in this study was that controllable preparation of Co-modified Ni_xMg_yO with low cobalt content (= 2wt%) could improve catalytic performance mainly via promotion of WGS reaction.

Table 2 Comparison of catalysts performance in the steam reforming of HAc

Catalysts	Temp (℃)	*S/C*[a] (mol/mol)	*LHSV*[b] (h^{-1})	X_{HAc} (%)	H_2 yield (%)	Stability[c] (h)	Ref.
15wt% Ni + 2wt%Ru + CeO_x/Al_2O_3	750	3.18	21 (*W*)	100	74.6	> 10	[40]
0.38wt% Ru + $Mg(Al)O_x$	700	3.0	6 (*W*)	100	70	20	[41]
30wt% Ni + 8wt% K + Al_2O_3	600	1.5	12.1	95	75	> 30	[42]
18wt% Co + La/Al_2O_3	400	1.0	10.1	85	75	> 20	[43]
0.5wt% Rh + CeO_2-ZrO_2	650	3.0	47	90	80	15	[44]
8.2wt% Ni + 1.7wt% Co + MgO	700	3.0	61 (*W*)	99.1	86.9	> 30	This study

[a] *S/C* ratio is short for steam/carbon ratio.

[b] *LHSV* is short for liquid hourly space velocity, (*W*) indicates that the space velocity is stated as weight hourly space velocity (*WHSV*).

[c] Time for the conversion or H_2 yield decrease 10% of its initial value.

The spent catalysts were also tested to study carbon deposition. Fig. 6 (a) shows results of the thermogravimetric analysis of the four spent catalysts after 30 h reaction. The weight loss of catalysts was primarily attributed to the combustion of the deposited carbon in a temperature range of 400-700 ℃.[45] The total weight losses of the spent catalysts were found in the order of Ni_xMg_yO-2Co (4.1wt%) < Ni_xMg_yO (15.6wt%) < Ni_xMg_yO-4Co (33.1wt%) < Ni_xMg_yO-6Co (45.1wt%). This sequence is also consistent with the result of durability test that the Ni_xMg_yO-2Co catalyst showed the best performance, while the Ni_xMg_yO-4Co and Ni_xMg_yO-6Co catalysts suffered quick deactivation. This indicates that the carbon deposition can be the main cause of catalytic deactivation in these steam reforming experiments.

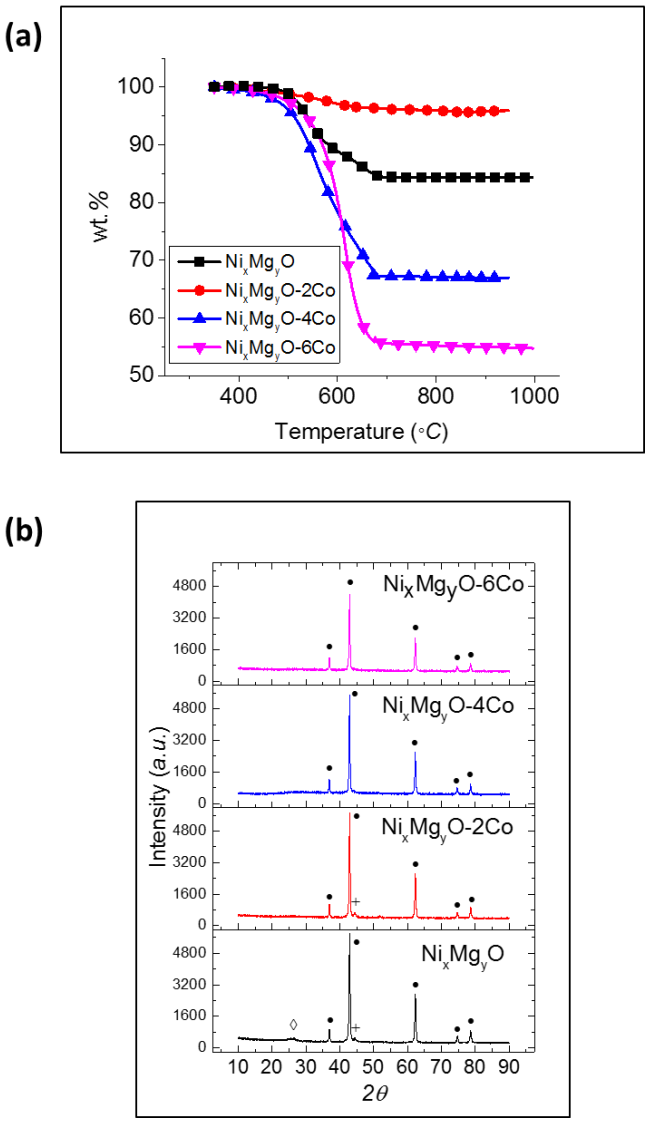

Fig. 6. (a) Thermogravimetric analysis profiles of the spent catalysts after 30 h steam reforming of acetic acid; (b) X-ray diffraction patterns of the spent catalysts (●: NiO/MgO, +: Ni^0, ◊: ordered carbon).

For the Co-modified catalysts, the addition of the second active compound Co accelerated the gasification of the carbon deposition precursors.[39] However, the excessive of Co content led to a strong affinity establishment between Ni and Co, which even weakened the carbon removal. This affinity was confirmed with the H_2-TPR profile that the reducibility of the catalysts decreased with increasing of cobalt doping weight. On the other hand, this affinity was also proved by the XRD patterns of the spent catalysts, shown in Fig. 6 (b). The spent Ni_xMg_yO and the Ni_xMg_yO-2Co catalysts were the only two catalysts which showed peaks in the range of 44.6-44.8°. These new formed diffraction peaks can be identified as Ni or Co metal.[46] However, the nickel and cobalt ions inside the MgO lattice

of the Ni_xMg_yO-4Co and Ni_xMg_yO-6Co catalysts were much more difficult to be activated by H_2 atmosphere.

Steam reforming of model blend

In the study of steam reforming of model blend, only the unmodified Ni_xMg_yO and the Ni_xMg_yO-2Co catalysts were tested. Fig. 7 illustrates the performance of catalysts in terms of model blend conversion, hydrogen yields and carbonaceous gas yield for extended periods. The Ni_xMg_yO catalyst appeared to boost the conversion rate from 84.9 to 93.6% during the first 6 h and remained above 90% for another 40 h. After that, the conversion rate started to decline rapidly to 76.6% at the 75^{th} hour. A similar situation was found in the hydrogen production where the H_2 yield climbed to 78.0% during the first 6 h and followed by a continuous decreasing to 53.0% after 75 h. Review the carbonaceous gas yield, CO_2 yield started to decline after several hours while CO yield increased at the very beginning and turned into decline after 40 h. For the CH_4 yield, it increased from 0.4% to roughly 5.5% and then kept relatively stable. In general, the catalytic activity of the Ni_xMg_yO increased at the beginning of the experiment due to the hydrogen activation of the residual Ni^{2+} or Co^{2+}. The decline of CO_2 and increment of CO indicated the attenuation of WGS reaction, hence, the H_2 yield decreased rapidly while model blend conversion maintained above 90% for around 40 h. However, after that 40-50 h reaction, the overall performance of the Ni_xMg_yO catalyst started to rapidly deactivate, associated with decline of carbon conversion and the yields of H_2, CO and CO_2.

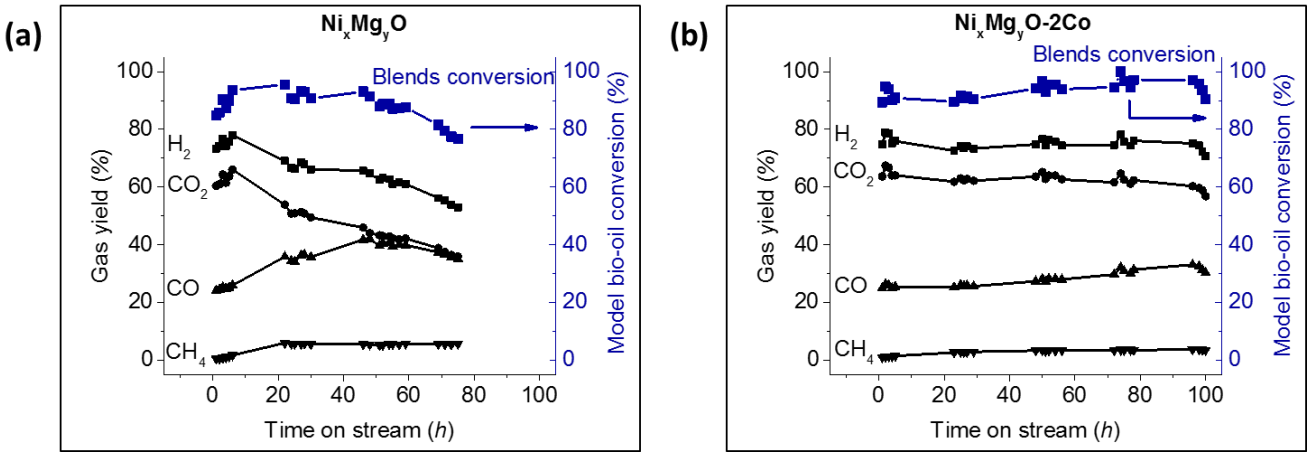

Fig. 7. Model blend conversion and gas yield profiles of catalysts as a function of time (reaction condition: P = 1 atm, $GHSV$ = 131,000 h^{-1}, S/C = 6, T = 800 ℃).

The Ni_xMg_yO-2Co catalyst (shown in Fig. 7 (b)) exhibited stable performance in carbon conversion within the region of 90-95% and hydrogen yield of above 70% for 100 h. Both the yields of CO_2 and CO were relative stable, which suggested the maintenance of the activity of WGS reaction. On the other hand, CH_4 yield of the Ni_xMg_yO-2Co catalyst was also kept below 3.5% in the whole time. Therefore, doping of 2 wt% Co not only greatly alleviate the suppression of WGS reaction, but also substantially expend lifetime of the Ni_xMg_yO catalyst due to improvement of its resistance to coking.

Conclusions

This research demonstrated that low cobalt doping on the Ni_xMg_yO solid solution catalysts promoted the initial H_2 yield in the steam reforming of HAc via the enhanced WGS reaction and the steam reforming of methane, which also alleviated the suppression of the exothermic WGS reaction at high temperatures (800 ℃). The high cobalt loading enhanced the affinity between Ni and Co and subsequently reduced the reducibility of the oxidized active components on the surface, which led to the deteriorated catalytic performance with a lower H_2 yield and HAc conversion. In addition, the Ni_xMg_yO-2Co was found exhibiting a desirable catalytic performance with no obvious deactivation in the durability test with final H_2 yield and HAc conversion rate reached 86.9% and 99.1%, respectively, which also demonstrated excellent performance in the reforming of model bio-oil blend.

Supporting information summary

The detailed experimental protocols, including catalytic performance test procedure, catalyst preparation, catalyst characterization, are provided in the supporting information.

Acknowledgements

Following funding bodies are acknowledged for partially sponsoring this research: Ningbo Science and Technologies Innovation 2025 Major Special Project (2018B10027). Ningbo Bureau of Science and Technology is acknowledged for its support under its Key Laboratory Scheme. The University of Nottingham Ningbo China is also acknowledged for IDIC scholarship providing scholarship to the first two authors.

Keywords

Acetic acid; Co-modified catalyst; Hydrogen production; Steam reforming; Water-gas shift reaction

References

[1] S. Czernik, R. French, ***Int. J. Hydrog. Energy.*** **2014**, *39*, 744-750.

[2] K. Raffelt, E. Henrich, A. Koegel, R. Stahl, J. Steinhardt, F. Weirich, ***Appl. Biochem. Biotechnol.*** **2006**, *129*, 153-164.

[3] D. Wang, D. Montané, E. Chornet, ***Appl. Catal. A-Gen***. **1996**, *143*, 245-270.

[4] J. R. Galdámez, L. García, R. Bilbao, ***Energy Fuels.*** **2005**, *19*, 1133-1142.

[5] M. Ferrandon, J. Mawdsley, T. Krause, ***Appl. Catal. A-Gen.*** **2008**, *342*, 69-77.

[6] R. M. Navarro, M. A. Peña, J. L. G. Fierro, ***Chem. Rev.*** **2007**, *107*, 3952-3991.

[7] J. Remón, J. A. Medrano, F. Bimbela, L. García, J. Arauzo, ***Appl. Catal., B.*** **2013**, *132-133*, 433-444.

[8] Z. Yu, X. Hu, P. Jia, Z. Zhang, D. Dong, G. Hu, S. Hu, Y. Wang, J. Xiang, ***Appl. Catal., B.*** **2018**, *237*, 538-553.

[9] Z. Zhang, X. Hu, J. Li, G. Gao, D. Dong, R. Westerhof, S. Hu, J. Xiang, Y. Wang, ***Fuel.*** **2018**, *217*, 389-403.

[10] J. Pu, K. Nishikado, N. Wang, T. T. Nguyen, T. Maki, E. W. Qian, ***Appl. Catal., B.*** **2018**, *224*, 69-79.

[11] A. Oasmaa, D. Meier, ***J. Anal. Appl. Pyrolysis.*** **2005**, *73*, 323-334.

[12] E. C. Vagia, A. A. Lemonidou, ***Int. J. Hydrog. Energy.*** **2007**, *32*, 212-223.

[13] C. Rioche, S. Kulkarni, F. C. Meunier, J. P. Breen, R. Burch, ***Appl. Catal., B.*** **2005**, *61*, 130-139.

[14] G. Chen, J. Tao, C. Liu, B. Yan, W. Li, X. Li, ***Renewable Sustainable Energy Rev***. **2017**, *79*, 1091-1098.

[15] K. Takanabe, K.-I. Aika, K. Inazu, T. Baba, K. Seshan, L. Lefferts, ***J. Catal.*** **2006**, *243*, 263-269.

[16] Z. Li, X. Hu, L. Zhang, S. Liu, G. Lu, ***Appl. Catal. A-Gen***. **2012**, *417–418*, 281-289.

[17] W. Nabgan, T. A. T. Abdullah, R. Mat, B. Nabgan, A. A. Jalil, L. Firmansyah, S. Triwahyono, **I*nt. J. Hydrog. Energy*. 2017**, *42*, 8975-8985.

[18] R. Trane, S. Dahl, M. S. Skjøth-Rasmussen, A. D. Jensen*, Int. J. Hydrog. Energy*. **2012**, *37*, 6447-6472.

[19] S. Rajadurai, ***Catal. Rev***. **1994**, *36*, 385-403.

[20] Y. Choi, H. G. Stenger, ***J. Power Sources***. **2003**, *124*, 432-439.

[21] D. Li, L. Zeng, X. Li, X. Wang, H. Ma, S. Assabumrungrat, J. Gong, ***Appl. Catal., B***. **2015**, *176–177*, 532-541.

[22] B. Dou, Y. Song, C. Wang, H. Chen, Y. Xu, ***Renewable Sustainable Energy Rev***. **2014**, *30*, 950-960.

[23] D.-W. Lee, M. S. Lee, J. Y. Lee, S. Kim, H.-J. Eom, D. J. Moon, K.-Y. Lee, ***Catal. Today***. **2013**, *210*, 2-9.

[24] L. He, H. Berntsen, E. Ochoa-Fernández, J. C. Walmsley, E. A. Blekkan, D. Chen, ***Top. Catal***. **2009**, *52*, 206-217.

[25] W. Nabgan, T. A. T. Abdullah, R. Mat, B. Nabgan, A. A. Jalil, L. Firmansyah, S. Triwahyono, ***Int. J. Hydrog. Energy***. **2017**, *42*, 8975-8985.

[26] L. A. Garcia, R. French, S. Czernik, E. Chornet, ***Appl. Catal. A-Gen***. **2000**, *201*, 225-239.

[27] K. K. Pant, P. Mohanty, S. Agarwal, A. K. Dalai, ***Catal. Today***. **2013**, *207*, 36-43.

[28] F. Zhang, N. Wang, L. Yang, M. Li, L. Huang, ***Int. J. Hydrog. Energy***. **2014**, *39*, 18688-18694.

[29] P. Lan, Q. Xu, M. Zhou, L. Lan, S. Zhang, Y. Yan, ***Chem. Eng. Technol***. **2010**, *33*, 2021-2028.

[30] K. W. Sing, ***J Porous Mater***. **1995**, *2*, 5-8.

[31] Y. H. Hu, E. Ruckenstein, ***Catal. Lett***. **1997**, *43*, 71-77.

[32] S. Tang, J. Lin, K. L. Tan, ***Catal. Lett***. **1998**, *51*, 169-175.

[33] P. Chen, H.-B. Zhang, G.-D. Lin, K.-R. Tsai, ***Appl. Catal. A-Gen***. **1998**, *166*, 343-350.

[34] X. Luo, Y. Hong, F. Wang, S. Hao, C. Pang, E. Lester, T. Wu, ***Appl. Catal., B***. **2016**, *194*, 84-97.

[35] M. Yu, K. Zhu, Z. Liu, H. Xiao, W. Deng, X. Zhou, ***Appl. Catal., B***. **2014**, *148–149*, 177-190.

[36] W. Cai, P. R. d. l. Piscina, K. Gabrowska, N. Homs, ***Bioresour. Technol***. **2013**, *128*, 467-471.

[37] M.-S. Fan, A. Z. Abdullah, S. Bhatia, ***Appl. Catal., B***. **2010**, *100*, 365-377.

[38] X. Yang, Y. Wang, M. Li, B. Sun, Y. Li, Y. Wang, ***Energy Fuels***. **2016**, *30*, 2198-2203.

[39] C. H. Bartholomew, ***Appl. Catal. A-Gen***. **2001**, *212*, 17-60.

[40] J. Pu, F. Ikegami, K. Nishikado, E. W. Qian, ***Int. J. Hydrog. Energy***. **2017**, *42*, 19733-19743.

[41] F. Bossola, C. Evangelisti, M. Allieta, R. Psaro, S. Recchia, V. Dal Santo, ***Appl. Catal., B***. **2016**, *181*, 599-611.

[42] X. Hu, G. Lu, ***Green Chem***. **2009**, *11*, 724-732.

[43] X. Hu, G. Lu, ***Catal. Commun***. **2010**, *12*, 50-53.

[44] E. C. Vagia, A. A. Lemonidou, ***J. Catal***. **2010**, *269*, 388-396.

[45] K. Tomishige, Y.-g. Chen, K. Fujimoto, ***J. Catal.*** **1999**, *181*, 91-103.

[46] T. Furusawa, A. Tsutsumi, ***Appl. Catal. A-Gen.*** **2005**, *278*, 207-212.

Table of Contents

The Ni_xMg_yO solid solution with low cobalt doping (Co loading = 2wt%) achieved an excellent and stable H_2 yield in a 30-hour test at 700 °C. Co promotes the initial H_2 yield in the steam reforming of HAc mainly due to the enhanced WGS reaction. However, higher cobalt loading enhanced the affinity between Ni and Co and subsequently reduced the reducibility of the oxidized active components on the surface, which led to the deteriorated catalytic performance.